Supplementary Information

For

FRAME v1.0: Advancing Fire Risk Assessment in Tropical Fragmented Forests with a Machine Learning Environment

Barik, Anasuya [1]*; *Baidya Roy, Somnath* [1]

[1] *Indian Institute of Technology Delhi, Hauz Khas, New Delhi, India*

* *Correspondence to*: Anasuya Barik (Anasuya.Barik@cas.iitd.ac.in)

Annexure 1: Spin-up of intermediate indices

The FFMC, DMC and DC of a particular day depend on the values of these indices in the previous day. Typically the first day of the simulation is started by initializing the FFMC, DMC and DC with the default values of 85, 6 and 15 respectively. Since the typical values of these indices are much higher in the tropical regions, we performed 12 experiments in three sets to determine the time required by the system to produce stable values of FFMC, DMC and DC. All of these experiments were of a three-year duration wherein different combinations of initialization values of FFMC, DMC and DC were provided to the 1st January of the first year. In the second and third years, the simulated values of FFMC, DMC and DC of 31st December in the previous year were provided as initialization. We provided the model with daily climatology values of meteorological inputs for all years. In the first set of experiments, the code was initialized with FFMC values of 75, 80, 85 and 90. The DMC and DC were initialized with the default values of 6 and 15. In the second set, we initialized the FFMC and DC with default values and varied the DMC initialization with values 6, 50, 100, and 150. In the third set, DC initialization was varied with values 15, 50, 100, and 150.

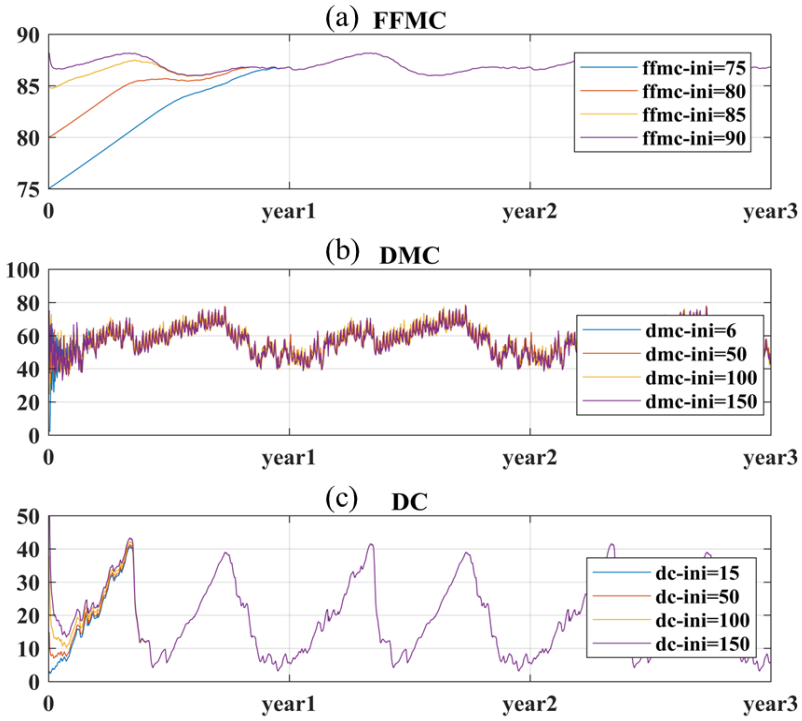

(Figure S1: Spin-up simulation for (a) FFMC, (b) DMC, and (c) DC)

In all conducted experiments, we observed that intrannual variability in DMC is the most pronounced, followed by DC, with the lowest variability observed in FFMC. From the first set of experiments, we see that irrespective of the initialization value of FFMC, the curve stabilizes after year 1 (Figure S1.a). For DMC (Figure S1.b), curves with different initialization values start to converge from day 70, although they do not perfectly align. In the case of DC we observe a bimodal signature annually and the curves with different DC initializations converge around day 150 of year 1. Overall, all the three intermediate indices converge by year 1 leading us to conservatively conclude that the CFFDRS FWI consistently produces stable output irrespective of the initial values of FFMC, DMC, and DC. This aligns with the findings reported by Barik & Baidya Roy, (2023), even though they utilized different meteorological inputs and a different approach to determine the spin-up period. In summary, regardless of the input meteorological dataset and the initial values, the CFFDRs should be spun-up for at least a year for reliable outputs.

Annexure 2: Suitability of CFFDRS for Indian forest regions

To test if the CFFDRS can be used in Indian forest regions under Indian weather conditions, we compared the responses of the system when driven by idealized meteorological drivers and when driven by observed meteorological data. For this purpose, we performed sensitivity experiments by gradually increasing values of one meteorological drivers while keeping the other drivers at a constant value. These experiments are listed in table 1. For all the three a, b, and c sets, the experiments were done for two rainfall conditions, precipitation = 0 mm and precipitation = 10 mm. Because forest fire

occurs mostly under dry conditions, we did not use any higher precipitation values. The FWI values from these idealized sensitivity experiments were compared to the FWI calculated when the CFFDRS was driven by observed ERA5 data.

For this purpose, the ERA5-driven simulated FWIs were binned into conditions similar to the idealized experiments. For example, in experiment set a (i), FWI was computed at pixels having relative humidity in bins such as <20%, 20-40%, 40-60%, 60-80%, and 80-100%, wind speed 10kmph and no precipitation. Since this experiment tested the variability of FWI with temperature, we retained the temperature of these pixels. In this way, the FWI responses from all setups similar to ideal experiments were calculated and plotted as functions of the relevant meteorological drivers, and their patterns were analyzed. The outcomes of this suitability assessment is described in the results section.

Table S1: Sensitivity experiments for assessing ideal CFFDRS behaviour

	2m Temperature	**Relative Humidity**	**Wind speed**	**Precipitation**
Experiment set (a)	(i) Varying from 0-100°C	20, 40, 60, 80, 100%	10 kmph	prec=0
	(ii) Varying from 0-100°C	20, 40, 60, 80, 100%	10 kmph	prec=10 mm
Experiment set (b)	(ii) 10, 20, 30, 40, 50°C	Varying from 0-100%	10 kmph	prec=0
	(ii) 10, 20, 30, 40, 50°C	Varying from 0-100%	10 kmph	prec=10 mm
Experiment set (c)	(ii) 10, 20, 30, 40, 50°C	10%	Varying from 0-50 kmph	prec=0
	(ii) 10, 20, 30, 40, 50°C	10%	Varying from 0-50 kmph	prec=10 mm

The families of curves (Figure S2) representing the idealized behaviour of the FWI model depict the impacts of varying weather parameters on FWI. The figure shows that FWI increases with an increase in temperature and wind speed but decreases with increasing relative humidity (Figure 4 i(a), i(b), i(c), iii(a), iii(b), iii(c)). A warm atmosphere helps ignite and burn fuel faster as less heat energy would be used to raise the fuels to their ignition temperature (Flannigan et al., 2000; Wotton & Flannigan, 1993). At lower relative humidity, we see a steeper curve of FWI increasing with increasing temperature. The temperature rise also contributes to a decrease in relative humidity, hence the FWI is affected by the individual variables as well as their interdependence (Countryman, 1972). Unshaded fuels experiencing warmer and drier atmospheres are more susceptible to causing more intense fires if ignited (Scheiter et al., 2015). At very high relative humidity or when precipitation occurs, the available fuel becomes saturated with moisture (Dimitrakopoulos & Papaioannou, 2001) and under such conditions, FWI is very low and does not change with any change in temperature. With steadily increasing relative humidity, the evaporation rate of moisture from the fuel surface is affected thus increasing the fuel moisture and decreasing FWI values. Drier atmospheres lead to a fire favourable conditions in which a fire is likely to ignite easily and burn more vigorously (Cruz et al., 2012). Wind speed primarily affects the FFMC and

ISI indices (Arnell et al., 2021; Field, 2020). Increased wind leads to more evaporation from damp surfaces by carrying away moist air and bringing in dryer air. When the fire is ignited, the wind increases the supply of oxygen and facilitates the combustion process (Santoso et al., 2019). In the ideal experiments, it was observed that with uniformly increasing wind speed, FWI increases, and warmer and drier conditions increase the slope of this variation. These characteristic patterns were observed even when the FWI was computed with ERA5 forcing over India (Figure S2 column (ii) and (iv)).

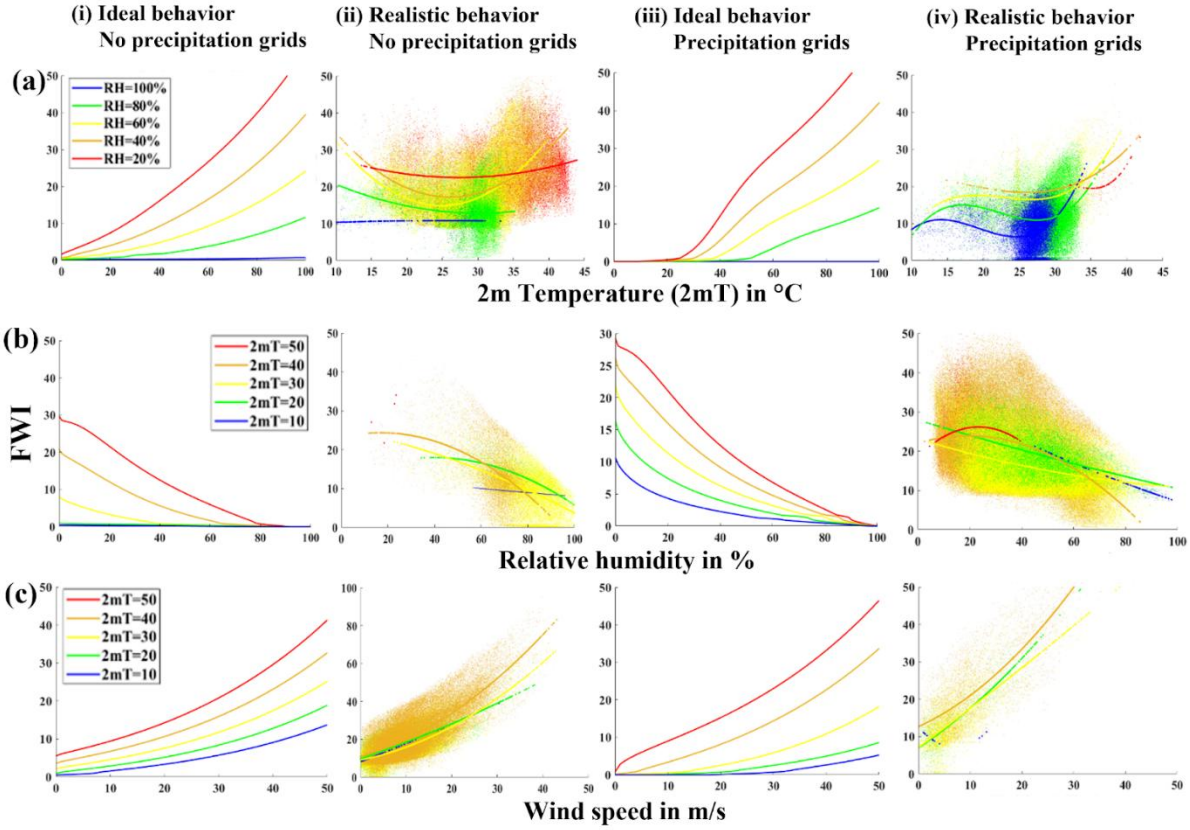

Figure S2: Idealistic (i and iii) and realistic (ii and iv) model performance with Indian Climate for varying (a) temperature, (b) relative humidity, and (c) wind speed for (i and ii) no precipitation grids and (iii and iv) precipitation occurring grids respectively.

Annexure 3: Methods to calculate FWI thresholds for fire danger classes

1. Percentile based

Following Barik & Baidya Roy, (2023) and a method used by the U.S. Forestry Services, we first considered thresholds of 22nd, 45th, 90, and 97th percentile FWI as the upper threshold values for Low, Medium, High, and Very high danger classes respectively. Then to further refine these thresholds we plotted the Receiver Operating Characteristics (ROC) curve in these intervals. ROC curve is a tool used to find out the best classifier in categorical problems (Figure S3(a)). In a given interval, it plots a curve between the True Positive Rate (TPR) and the False Positive Rate (FPR) at varying decision thresholds. The point in the curve closest to the (1,0) point marks the best operating point. In this case, we first

selected the interval between 0th and 22nd percentile. Considering all consecutive values between 0-22 as the decision threshold, we plotted the ROC curve and determined the best operating point which was closest to (1,0) point. This was the threshold value of that interval. This process was then repeated for the other intervals and all the zones. Thus, instead of the threshold values at the 22nd, 45th, 90th, and 97th percentile, we selected the best classifier percentile values in that interval using the ROC curve.

2. Percentage of fire events based

In this method, we computed the percentage of fires occurring beyond every percentile index (PI) of FWI and applied hierarchical clustering to classify the dataset into 5 clusters. Hierarchical clustering (Nielsen, 2016) is an unsupervised learning method that is used to divide data points based on similarity in attributes and patterns. Here, we have used agglomerative hierarchical clustering, where data points start as individual clusters and are successively merged to form larger clusters. Hierarchical clustering is implemented by calculating distances between data points, which in our case is the percentage of fires corresponding to each PI. Then it iteratively merges clusters based on these distances. The process continues until a desired level of detail or structure is achieved. We computed the highest percentage of fires in the 5 clusters and computed the corresponding FWI and PI as thresholds for each class (Figure S3(b)).

3. Logistic regression based

Logistic regression is another method that computes the probability of occurrence in problems with two possible outcomes (DeMaris, 1995). In this study, we use logistic regression to model the likelihood of fire occurrence at the daily scale. The outcome variable is binary, where a grid cell is assigned a value of 1 if a fire occurred on a given day and 0 otherwise. Barik & Baidya Roy, (2023) considered 0.2, 0.5, 0.7 and 0.9 as the danger class thresholds. As these threshold values were subjective in nature, to make the thresholds more robust, we used hierarchical clustering. We first fitted a binomial logistic regression model to our combined fire-presence and fire-absence observations against their corresponding FWI values. This produced a probability of fire occurrence for each FWI. We then drew a random sample of 1,000 predicted probabilities and applied hierarchical clustering (Ward's linkage) to group them into five clusters. For each cluster, we identified the highest probability value and mapped it back to its position in the sorted FWI array. These mapped FWI values became the thresholds which we overlaid on the logistic sigmoid curve (Figure S3(c)).

4. K-means clustering

We used the K-Means clustering method as in Barik & Baidya Roy, (2023). First, we paired each FWI percentile value with its corresponding fire-count and arranged these as a two-column dataset. We then applied k-means clustering (k = 5, maximum 1,00,000 iterations) to group the data into five clusters. K-means is an unsupervised algorithm that assigns each point to the nearest cluster centroid and iteratively adjusts centroids to minimize the total within-cluster variance. After clustering, we sorted the centroids by their FWI coordinate and took these values as the thresholds of the danger classes. Finally, we overlaid these FWI thresholds on the FWI–fire count per percentile curve (Figure S3d).

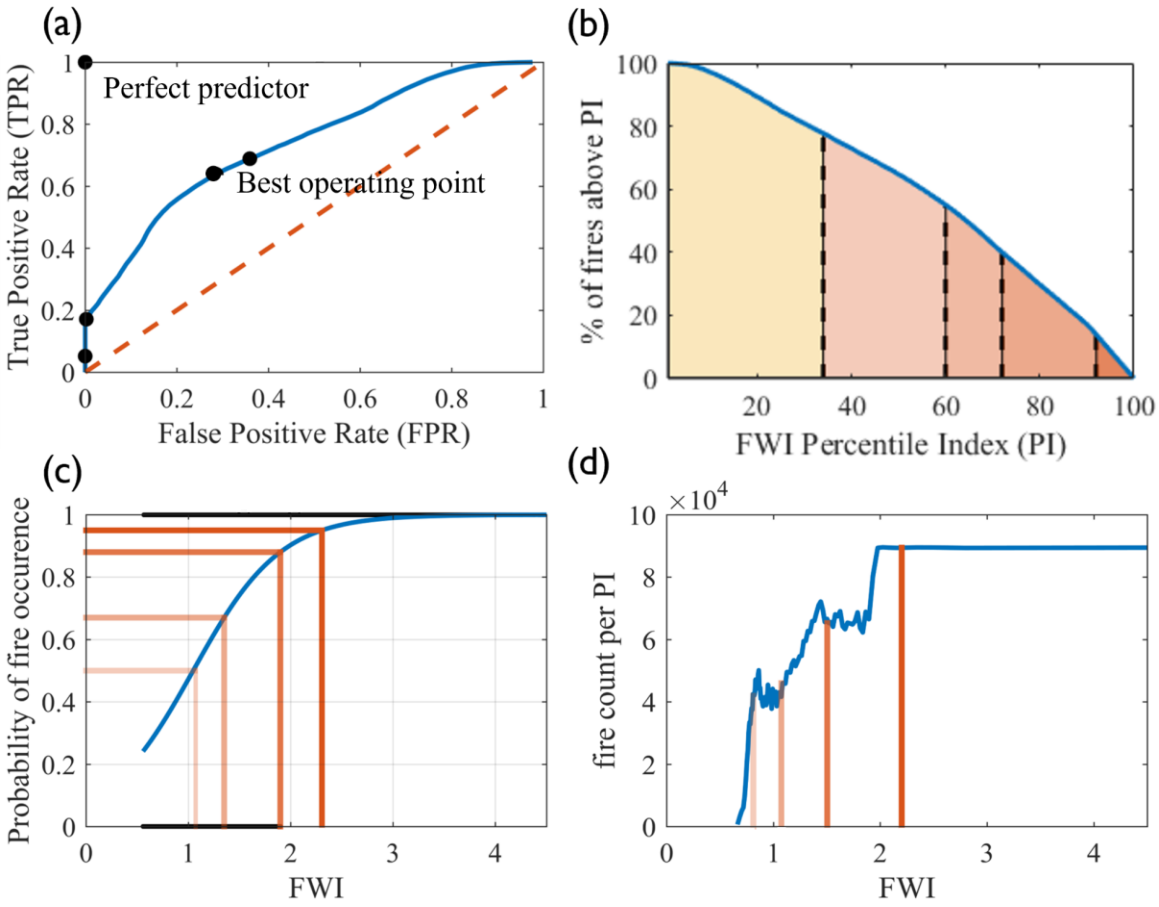

Figure S3: Graphical illustration of (a) ROC curve of the percentile-based method, thresholds in (b) percentage method, (c) logistic regression method, and (d) K-means clustering method in the NE zone. We obtain similar graphs in other zones also.

Annexure 4: Details on the evaluation of FDRS thresholds

To evaluate the performance of the FDRS thresholds, we analysed various skill metrics and robustness checks. We ensured that the following three criteria were met:

- Minimum/ no overlap between the classes when considering different methods.
- Increase in the fire occurrence probability with each class.
- Acceptable values of evaluative parameters like critical success rate (CSI; Schaefer, 1990), probability of detection (hit rate), and false alarm ratio (FAR; Schaefer, 1990), hits due to chance and correct rejection. To assess these parameters, we considered the Low danger class threshold as a benchmark for the confusion matrices for each zone. These parameters were calculated using the following equations:

1. Critical Success Index (CSI):

$$CSI = \frac{Hits}{Hits + Misses + False\ alarms}$$

2. Probability of Detection (Hit Rate):

$$Hit\ Rate = \frac{Hits}{Hits + Misses}$$

3. False Alarm Ratio (FAR):

$$FAR = \frac{False\ alarms}{False\ alarms + Correct\ rejections}$$

4. Hits due to Chance:

$$Hits\ due\ to\ chance = \frac{Total\ events\ x\ Total\ Hits}{Total\ observation2}$$

5. Correct Rejection:

$$Correct\ rejection = \frac{Correct\ rejections}{Correct\ rejections + False\ alarms}$$

Annexure 5:

Table S2: Performance statistics of various machine learning and neural network predictive models to simulate fire count

ML Models	**HIM**		**NE**		**CEN**		**DEC**		**WG**	
	R-squared	RMSE	R-squared	RMSE	R-squared	RMSE	R-squared	RMSE	R-squared	RMSE
Interactions linear	0.51	238	0.41	1059	0.29	440	0.6	331	0.25	207
Complex tree	0.68	193	0.62	849	0.65	307	0.74	262	0.17	211
Fine Gaussian SVM	0.33	281	0.63	844	0.41	399	0.47	379	0.2	214
Rational quadratic GPR	0.71	185	0.66	804	0.66	303	0.78	245	0.44	179

Squared exponential	0.73	179	0.61	868	0.49	373	0.79	239	0.42	176
Bagged/boosted trees	0.76	169	0.72	733	0.68	295	0.77	250	0.36	185
ANN based	0.85	181	0.8	877	0.73	415	0.89	232	0.71	167